Journal of Organometallic Chemistry 878 (2018) 77–83

Contents lists available at ScienceDirect

Journal of Organometallic Chemistry

journal homepage: www.elsevier.com/locate/jorganchem

The coordination and activation of azobenzene by $Ru_5(\mu_5\text{-}C)$ cluster complexes

Richard D. Adams*, Humaiara Akter, Mark D. Smith, Jonathan D. Tedder

Department of Chemistry and Biochemistry, University of South Carolina, Columbia, SC, 29208, USA

ARTICLE INFO

Article history:
Received 14 September 2018
Received in revised form
8 October 2018
Accepted 9 October 2018
Available online 11 October 2018

Dedicated to Professor Richard J. Puddephatt for his many pioneering contributions to the field of organometallic chemistry on the occasion of his 75th birthday.

Keywords:
Ruthenium cluster
Aromatic CH activation
Azobenzene
Electronic unsaturation
Crystal structure

ABSTRACT

The reaction of $Ru_5(\mu_5\text{-}C)(CO)_{15}$, **1** with azobenzene, PhN = NPh, yielded the pentaruthenium carbido cluster compound $Ru_5C(CO)_{13}(C_6H_4N{=}NC_6H_5)[\mu\text{-}H]$, **4** containing a chelating *ortho*-metalated azobenzene ligand on one of the ruthenium atoms in a opened square-pyramidal Ru_5C cluster. Compound **4** is electronically unsaturated and it readily adds one CO ligand at 25 °C to yield the electronically saturated complex $Ru_5C(CO)_{14}(C_6H_4N{=}NC_6H_5)[\mu\text{-}H]$, **5**. $Ru_5C(CO)_{13}(\mu\text{-}\eta^2\text{-}Ph)[\mu\text{-}Au(NHC)]$, **3** reacts with azobenzene to yield the azobenzene complex $Ru_5C(CO)_{13}(\mu{-}\eta^2{-}PhN{=}NPh)(\eta^1{-}Ph)[\mu{-}Au(NHC)]$, **6**, NHC = 1,3-bis(2,6-diisopropylphenyl-imidazole-2ylidene), which contains a novel bridging di-σ-η^2-*N*,*N*-coordinated azobenzene ligand across an open edge of an Ru_5C cluster. Compound **6** eliminated benzene and was transformed to the new compound $Ru_5C(CO)_{13}(C_6H_4N{=}NC_6H_5)[\mu{-}Au(NHC)]$, **7** when heated to 105 °C for 3 h. Compound **7** is similar to **4** except that it has an Au(NHC) group in the place of the bridging hydrido ligand in **4**. Compound **7** is also formally electronically unsaturated like **4**. All of the new compounds were characterized by single-crystal X-ray diffraction analyses. The structures, bonding and reactivity of the complexes are discussed.

1. Introduction

Azobenzene, PhN = NPh, has attracted attention for its interesting photoisomerization properties [1] and applications ranging from those of molecular devices [2] to pharmacology [3]. Azobenzene readily undergoes *ortho*-metallation at its phenyl rings when it is coordinated to metal complexes [4] and today it can be easily functionalized at these *ortho*-positions catalytically [5]. There are only a few structurally characterized examples of azobenzene ligands in polynuclear metal carbonyl cluster complexes [6].

In recent studies, we have been investigating the reactions of the pentaruthenium carbonyl cluster complex $Ru_5(\mu_5\text{-}C)(CO)_{15}$, **1** with molecules containing C-Au [7] and C-H bonds [8]. For example, we have shown that the pentaruthenium cluster complex **1** is able to activate the formyl C-H bond of *N*,*N*-dimethylformamide and certain aldehydes to yield the complexes $Ru_5(\mu_5\text{-}C)(CO)_{14}(\mu\text{-}\eta^2\text{-}O{=}CR)(\mu\text{-}H)$, R = NMe_2, Ph, cinnamoyl, furanyl that contain a bridging acyl ligand formed by opening of the Ru_5C square pyramidal cluster of metal atoms via oxidative addition of the formyl C-H bond to the metal atoms, eq. (1) [7].

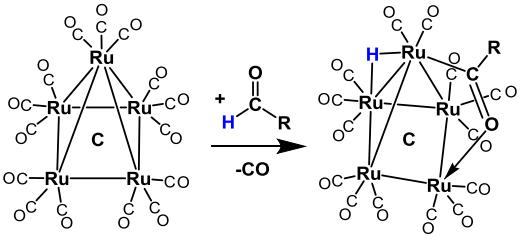

$Ru_5(C)(CO)_{15}$, **1**

(1)

Compound **1** also reacts with (NHC)AuPh to yield the $AuRu_5$ complexes, $Ru_5C(CO)_{14}(Ph)[\mu\text{-}Au(NHC)]$, **2** and $Ru_5C(CO)_{13}(\mu\text{-}\eta^2\text{-}Ph)[\mu\text{-}Au(NHC)]$, **3**, NHC = dippim, by activation of the Au-C bond to the phenyl ring [9].

* Corresponding author.
E-mail address: ADAMSRD@mailbox.sc.edu (R.D. Adams).

https://doi.org/10.1016/j.jorganchem.2018.10.004
0022-328X/

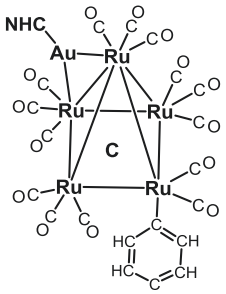

2

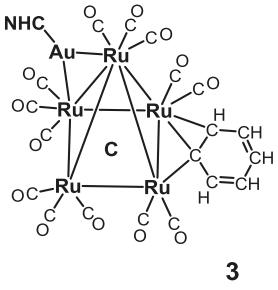

3

We have now investigated the reactions of **1** and **3** with azobenzene. We have obtained the first pentaruthenium complexes containing azobenzene ligands. *Ortho*-metallation at one of the phenyl rings has been observed. Two of the new complexes possess an unusual and unexpected electronic unsaturation which affects their structures and reactivity. The results of these studies are reported herein.

2. Experimental section

General Data. All reactions were performed under nitrogen atmosphere by using standard Schlenk techniques. Reagent grade solvents were dried by the standard procedures and were freshly distilled prior to use. Infrared spectra were recorded on a Thermo Fisher Scientific Nicolet iS10 FT-IR spectrophotometer. ^{1}H NMR spectra were recorded on a Varian Mercury 300 spectrometer operating at 300.1 MHz for compounds **5**, **6** and **7**. ^{1}H NMR spectra for compound **4** was recorded on a Bruker AVANCE III spectrometer operating at 400 MHz. Mass spectrometric (MS) measurements performed by a direct-exposure probe using electron impact ionization (EI) were made on a VG 70S instrument for compounds **4** and **5**. Positive/negative ion mass spectra were recorded on a Micromass Q-TOF instrument by using electrospray (ES) ionization for compounds **6** and **7**. Azobenzene was purchased from KODAK and was used without further purification. $Ru_5C(CO)_{15}$, **1** [10] and $Ru_5C(CO)_{13}(\mu-\eta^2-Ph)[\mu-Au(NHC)]$, **3**, NHC = 1,3-bis(2,6-diisopropylphenyl-imidazole-2ylidene) [9] were prepared according to previously reported procedures. Reaction products were separated by TLC in the air on Analtech 0.25 and 0.5 mm silica gel 60 Å F_{254} glass plates.

2.1. Synthesis of $Ru_5C(CO)_{13}(C_6H_4N{=}NC_6H_5)(\mu$-H), 4

A 59.2 mg amount of **1** (0.0631 mmol) was dissolved in heptane in a 100 mL three-neck flask. 57.5 mg of azobenzene (0.3155 mmol) was then added to the solution which was then heated to reflux for 21 h. The reaction was monitored by IR spectroscopy. The solvent was then removed *in vacuo* and the product was isolated by TLC by using a hexane to methylene chloride solvent mixture to yield 20.5 mg of $Ru_5C(CO)_{13}(C_6H_4N{=}NC_6H_5)(\mu$-H), **4** (yield 27%). Spectral Data for **4**: IR νCO (cm^{-1} in hexane): 2094(m), 2063(s), 2059(vs), 2044(m), 2022(m), 2007(m), 1998(w), 1991(w), 1969(w). ^{1}H NMR (CD_2Cl_2, in ppm) δ = 8.29 (d, J = 7.5 Hz, 1H, Ph), 8.07 (d, J = 7.5 Hz, 2H, Ph), 7.46 (d, J = 7.5 Hz, 2H, Ph), 7.16 (dt, J = 8 Hz, 2H, C_6H_4), 7.16 (d, J = 3 Hz, 1H, C_6H_4), 7.16 (d, J = 3 Hz, 1H, C_6H_4), −22.25 (s, 1H, Ru-**H**). EI+/MS: m/z 1064 (M+). The isotope distribution pattern was consistent with the presence of five ruthenium atoms.

2.2. Synthesis of $Ru_5C(CO)_{14}(C_6H_4N$-$NC_6H_5)(\mu$-H), 5

1.9 mg of compound **4** was dissolved in 3–4 drops of benzene and 1 mL of heptane was added in a 20 mL glass vial. CO gas was bubbled through the solution slowly. A rapid color change from orange to yellow was observed. The vial was then stored under CO atmosphere at room temperature while the orange colored crystals were deposited overnight to yield 1.9 mg of $Ru_5C(CO)_{14}(C_6H_4N{=}NC_6H_5)(\mu$-H), **5** (yield 97%). Spectral Data for **5**: IR νCO (cm^{-1} in hexane): 2097(w), 2066(s), 2060(vs), 2047(m), 2033(w), 2024(w), 2015(w), 2001(w), 1991(vw), 1980 (vw). ^{1}H NMR (CD_2Cl_2, in ppm) d = 8.25 (dd, J = 8.4 Hz, 1H, Ph), 7.73–7.50 (m, 4H, Ph), 7.31–7.11 (m, 4H, C_6H_4), −21.78 (s, 1H, Ru-**H**). EI+/MS: m/z 1093 (M+) plus ions M$^+$ − n(CO), n = 1–14. The isotope distribution pattern was consistent with the presence of five ruthenium atoms.

2.3. Synthesis of $Ru_5C(CO)_{13}(\mu-\eta^2$-$PhN=NPh)(\eta^1-Ph)[\mu-Au(NHC)]$, 6

A 11.7 mg (0.0076 mmol) amount of **3** and 13.6 mg (0.0746 mmol) of azobenzene were dissolved in 25 mL heptane in a 50 mL three-neck flask and then heated to reflux with stirring for 11 h. The solution was then cooled and the solvent was removed *in vacuo*. The product was isolated by TLC by using a hexane to methylene chloride solvent mixture to yield 8.9 mg of $Ru_5C(CO)_{13}(\mu-\eta^2-PhN=NPh)(\eta^1-Ph)[\mu-Au(NHC)]$, **6** (yield 68%). Spectral Data for **6**: IR νCO (cm^{-1} in hexane): 2071(m), 2049(w), 2039(vs), 2030(s), 2026(m), 2015(w), 1996(m), 1980(w), 1969(w), 1962(w), 1953(w), 1938(vw). ^{1}H NMR (CD_2Cl_2, in ppm) δ = 7.32 (t, J = 8 Hz, 2H, para CC_2(i-Pr)$_2C_2H_2$C**H**, 7.29 (m, 7H, CC_2(i-Pr)$_2C_2$**H**$_2$CH + NPh), 6.97 (s, 2H, C(NC_6i-Pr$_2H_3$)C_2**H**$_2$, 6.9–5.6 (m, 12H, NPh), 2.70 (sept, J = 6.8 Hz, 4H, C**H**-(CH_3)$_2$), 1.16 (d, 6.8 Hz, J = 6 H, CH-(C**H**$_3$)$_2$), 1.15 (d, J = 6.8 Hz, 6 H, CH-(C**H**$_3$)$_2$), 1.01 (d, J = 6.8 Hz, 6 H, CH-(C**H**$_3$)$_2$),1.00 (d, J = 6.8 Hz, 6 H, CH-(C**H**$_3$)$_2$). ESI/MS: m/z 1750 (M + Na)$^+$.

2.4. Synthesis of $Ru_5C(CO)_{13}(C_6H_4N{=}NC_6H_5)[\mu Au(NHC)]$, 7

A 15.3 mg amount (0.0086 mmol) of **6** was dissolved in d_8-toluene in a NMR tube and was then heated to 105 °C for 3 h. The product $Ru_5C(CO)_{13}(C_6H_4N{=}NC_6H_5)[\mu-Au(NHC)]$, **7** was isolated by TLC by using a hexane to methylene chloride mixture to yield 2.8 mg of **7**, (yield 19%). Also 1.4 mg of **3** was isolated (yield 10.4%). Spectral data for **7**: IR νCO (cm^{-1} in hexane): 2072(vw), 2048(vs), 2039(w), 2031(m), 2015(m), 1998(m), 1991(w), 1955(vw). ^{1}H NMR (CD_2Cl_2, in ppm) δ = 8.25 (d, J = 8.7 Hz, 1H, Ph), 7.88 (d, J = 8.7 Hz, 2H, Ph), 7.43 (d, J = 8.7 Hz, 2H, Ph), 7.42 (d, J = 8.7 Hz, 2H, CC_2(i-Pr)$_2C_2H_2$C**H**), 7.29 (d, J = 7.8 Hz, 4H, CC_2(i-Pr)$_2$**C**$_2$**H**$_2$CH), 7.12 (s, 2H, C(NC_6i-Pr$_2H_3$)C_2**H**$_2$, 7.07 (dt, J = 7 Hz, 2H, C_6H_4), 6.84 (d, J = 7 Hz, 2H, C_6H_4), 6.82 (d, J = 7 Hz, 2H, C_6H_4), 2.78 (sept, 7 Hz, 4H, C**H**-(CH_3)$_2$), 1.37 (d, 7 Hz, 12 H, CH-(C**H**$_3$)$_2$), 1.13 (d, 7 Hz, 12H, CH-(C**H**$_3$)$_2$). ESI/MS: m/z 1649 (M+).

2.5. Crystallographic analyses

Single crystals of **4** (red), **5** (yellow-orange), **6** (brown), and **7** (orange-red) suitable for X-ray analyses were obtained by slow evaporation from a hexane/methylene chloride solvent mixture at room temperature. Crystals of compound **5** were grown from a solution in a heptane and benzene solvent mixture under a CO atmosphere. Each data crystal was glued onto the end of a thin glass fiber. For compounds **4**, **6** and **7**, X-ray intensity data were measured by using a Bruker SMART APEX CCD-based diffractometer by using Mo Kα radiation (λ = 0.71073 Å). The raw data frames were integrated by using the SAINT$^+$ program with a narrow-frame integration algorithm [11]. For compound **5** X-ray intensity data from a yellow-orange needle of approximate dimensions 0.03 × 0.06 × 0.16 mm^3 were collected at 100(2) K by using a Bruker D8 QUEST diffractometer equipped with a PHOTON-100

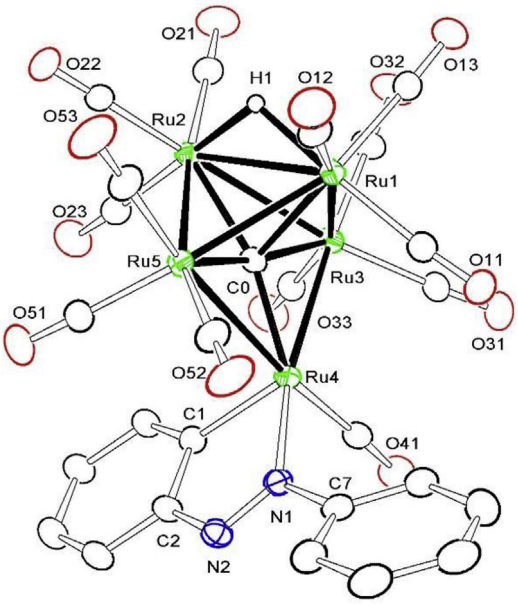

Fig. 1. An ORTEP diagram of the molecular structure of $Ru_5C(CO)_{13}(C_6H_4N{=}NC_6H_5)(\mu{-}H)$, **4** showing 20% thermal ellipsoid probability. Selected interatomic distances are (Å) as follow: Ru1-Ru3 = 2.8110(8), Ru1···Ru4 = 3.461(1), Ru1-Ru5 = 2.8236(8), Ru1-Ru2 = 2.8647(8), Ru2-Ru5 = 2.8314(8), Ru2-Ru3 = 2.8692(8), Ru3-Ru4 = 2.8952(8), Ru4-Ru5 = 2.8854(8), Ru1–H1 = 1.71(6), Ru2–H1 = 1.82(6), Ru1–Ru2 = 2.8647(8), Ru4–N1 = 2.087(5), Ru4–C1 = 1.992(6), N1–N2 = 1.273(7).

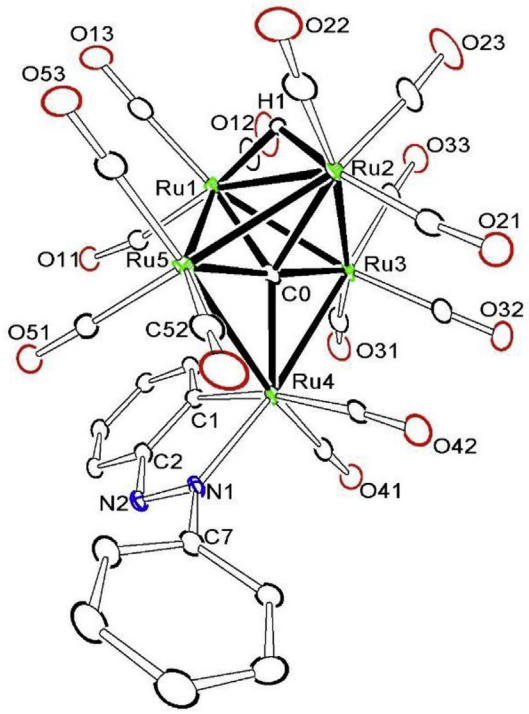

Fig. 3. An ORTEP diagram of the molecular structure of $Ru_5C(CO)_{14}(C_6H_4N{=}NC_6H_5)(\mu{-}H)$, **5** showing 25% thermal ellipsoid probability. Selected interatomic distances are (Å) as follow: Ru1-Ru5 = 2.8195(5), Ru1-Ru2 = 2.8338(5), Ru1-Ru3 = 2.9143(5), Ru1···Ru4 = 3.929(1), Ru2-Ru3 = 2.8298(5), Ru2- Ru5 = 2.8536(5), Ru3-Ru4 = 2.9254(5), Ru2···Ru4 = 3.980(1), Ru1-H1 = 1.71(4), Ru2-H1 = 1.71(4), Ru4-C41 = 1.894(4), Ru4-C42 = 1.952(4), Ru4-N1 = 2.072(3), Ru4-C1 = 2.111(4), Ru4-Ru5 = 2.9624(5), N1 - N2 = 1.279(4).

CMOS area detector and an Incoatec microfocus source (Mo Kα radiation, λ = 0.71073 Å) [12]. The data collection strategy consisted of seven 180° ω-scans at different φ settings and two 360° φ-scans at different ω angles, with a scan width per image of 0.5°. Corrections for Lorentz and polarization effects were also applied with SAINT+. Empirical absorption corrections based on the multiple measurements of equivalent reflections were applied by using the program SADABS. All structures were solved by a combination of direct methods and difference Fourier syntheses, and refined by full-matrix least-squares on F^2 by using the SHELXTL software package [13]. All non-hydrogen atoms were refined with anisotropic thermal parameters. Hydrogen atoms were placed in geometrically idealized positions and included as standard riding atoms during the least-squares refinements. Compound **4** crystallized in the monoclinic crystal system. The space group $P2_1/c$ was indicated for compound **4** based on the systematic absences in the data and was confirmed by the successful solution and refinement of the structure. Compound **5** also crystallized in the monoclinic crystal system. The space group *I*2/a (a nonstandard setting of *P*2/a) was used for the solution and refinement of this structure. Compounds **6** and **7** crystallized in the triclinic crystal system. The space group *P*-1 was assumed for the analyses of compounds **6** and **7**, and this was confirmed by the successful solution and refinement of both of these structures. Crystal data, data collection parameters and results of the analyses are summarized in Table S1.

2.6. Computational analyses

All molecular orbital calculations were performed with ADF2014 program by using the PBEsol-D3 functional with ZORA scalar relativistic correction [14] and valence triple-ζ+1 polarization, relativistically optimized (TZP) Slater-type basis set, with

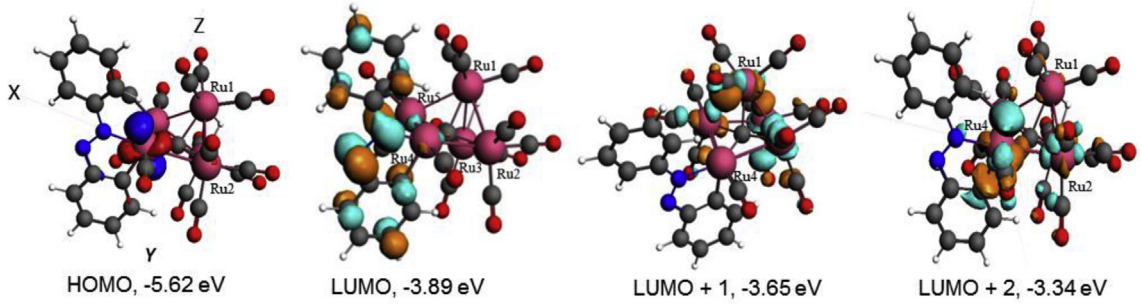

Fig. 2. Selected molecular orbitals (MOs) with calculated energies in eV for compound **4** that show the nature of the bonding between the metalated azobenzene ligand and the interactions of ruthenium atoms in the metal cluster. The ruthenium atoms are colored as pink. (For interpretation of the references to color in this figure legend, the reader is referred to the Web version of this article.)

small frozen cores. All computations were done by using the gas phase model. This choice of computational model is based on prior testing of various functionals and basis sets [15]. The PBEsolD3 functional, which was originally developed primarily for solids, was shown to be superior to other functionals in the PBE family in the structural parameters of large organic systems [16] and for metal clusters [17]. This is also consistent with our own testing of various functionals for the structures and relative energetics in organometallic cluster complexes [15]. The dispersion corrections by Grimme et al. were included upon additional testing, once they became available in the current release of ADF [14h]. All calculations were geometry-optimized and were initiated with the structures obtained from the crystal structure analyses.

3. Results and discussion

The reaction of **1** with azobenzene in a heptane solution at reflux 98 °C for 21 h yielded the new pentaruthenium carbido cluster compound $Ru_5C(CO)_{13}(C_6H_4N{=}NC_6H_5)(\mu\text{-}H)$, **4** in 27% yield. Compound **4** was characterized by IR and ^1H NMR spectroscopy, mass spectrometry and single-crystal X-ray diffraction analysis. An ORTEP diagram of the molecular structure of **4** is shown in Fig. 1. Compound **4** contains a chelating, *ortho*-metalated azobenzene ligand coordinated to an opened square-pyramidal Ru_5C cluster. The cluster can be described as a Ru_4C butterfly cluster that is bridged at the wingtips by the fifth Ru atom, Ru(4).

The atom Ru4 contains a chelating, cyclometalated azobenzene ligand which is coordinated by the nitrogen atom N1 and the metalated carbon atom C1, Ru4–N1 = 2.087 (5) Å, Ru4–C1 = 1.992 (6) Å. The N1 – N2 bond distance is typical of a N = N double bond, N1–N2 = 1.273(7) Å. The compound also contains one hydrido ligand H1 derived from the metalated phenyl ring. Atom H1 bridges the Ru1 – Ru2 metal – metal bond, Ru1–H1 = 1.71 (6) Å and Ru2–H1 = 1.82 (6) Å, $\delta = -22.25$. The metalated azobenzene ligand serves formally as a three electron donor. With a total of thirteen terminal CO ligands distributed as shown in Fig. 1, compound **4** contains a total of 74 cluster valence electrons which is two electrons less than the 76 electrons required for an 'open' Ru_5C cluster of five metal atoms [18]; thus, compound **4** is formally unsaturated by the amount of two electrons. Simpler electron counting procedures indicate that atom Ru4 has only 16 valence electrons. To try to obtain a better understanding of the electronic structure **4**, a geometry optimized PBEsolD3 ADF molecular orbital analysis of **4** was performed. Fig. 2 shows drawings of frontier orbitals in **4**. The highest occupied molecular orbital (HOMO) is dominated by a nonbonding d-orbital localized on the metal atom Ru4. This orbital is 65% a d_{xz}-orbital in the coordinate system that was assigned to the molecule in these calculations, see the MOs shown in Fig. 2. The

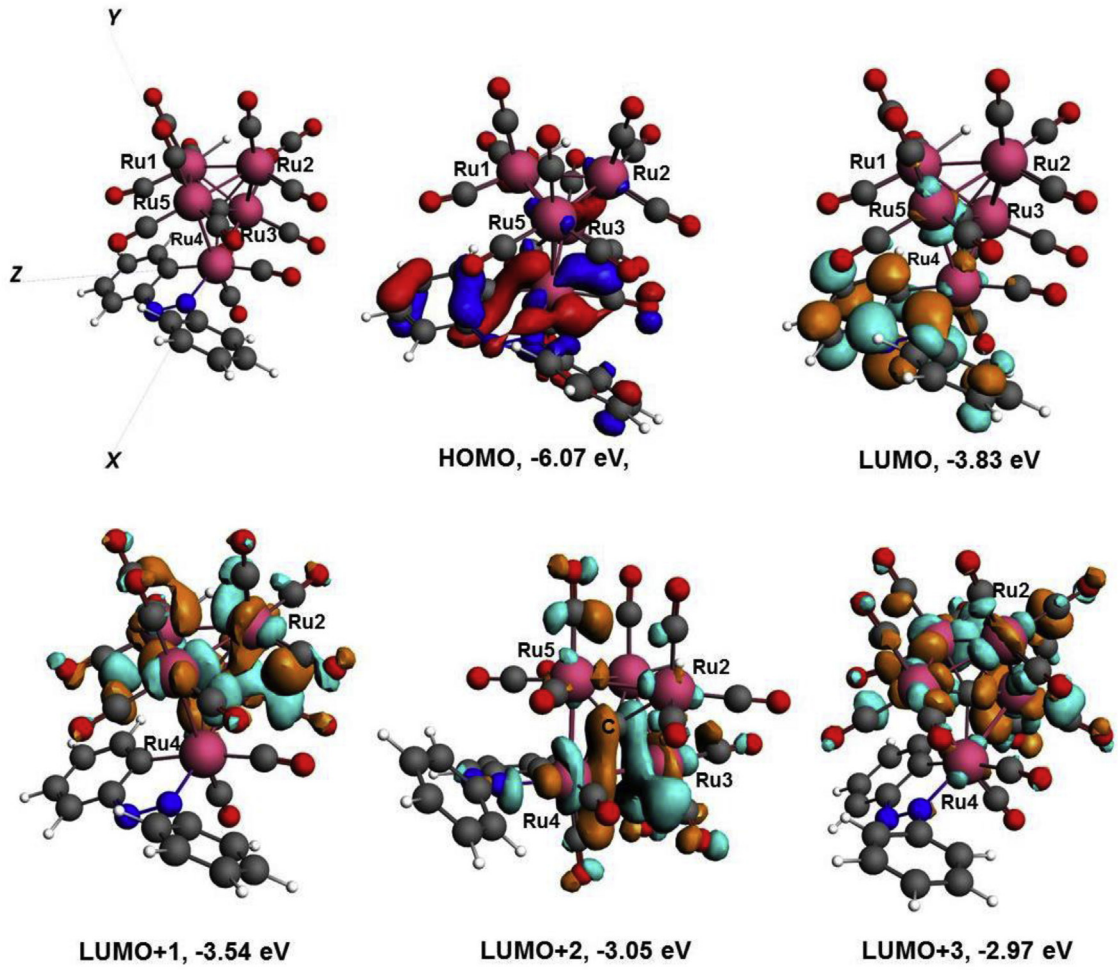

Fig. 4. Selected molecular orbitals (MOs) with calculated energies in eV for compound **5** that show the nature of the bonding between the metalated azobenzene ligand and the interactions of ruthenium atoms in the metal cluster. The ruthenium atoms are colored as pink. (For interpretation of the references to color in this figure legend, the reader is referred to the Web version of this article.)

lowest unoccupied molecular orbital (LUMO) is a delocalized π^*–orbital on the metalated azobenzene ligand. The LUMO+1 is a delocalized orbital on the Ru_4C portion of the cluster. The LUMO+2 is a very interesting empty orbital that is a hybrid composed of 13% d_z^2 and 8% p_z atomic orbitals in this model that is localized on Ru4. We believe that this orbital represents the "unsaturation" site on this metal atom. Curiously, although it is much longer than the normal Ru – Ru bond distances in the complex, Ru1-Ru3 = 2.8110(8) Å, Ru1-Ru5 = 2.8236(8) Å, Ru1-Ru2 = 2.8647(8) Å, Ru2-Ru5 = 2.8314(8) Å, Ru2-Ru3 = 2.8692(8) Å, Ru3-Ru4 = 2.8952(8) Å, Ru4-Ru5 = 2.8854(8) Å, the Ru1···Ru4 interatomic distance of 3.461(1) Å is much shorter than the corresponding Ru2···Ru4 distance of 4.030(1) Å in this molecule which is clearly a nonbonding interaction. Thus, there may be some significant long range attractive forces between the atoms Ru1 and Ru4. Electronic unsaturation can have important implications for the reactivity of metal complexes [19].

In order to test for unsaturation in compound **4**, we investigated the reaction of **4** with CO. A solution of **4** in a benzene-heptane solvent mixture was exposed to CO (1 atm) at 25 °C. The solution immediately changed color to yellow and the IR spectrum showed a complete conversion to a new compound subsequently confirmed to be $Ru_5C(CO)_{14}(C_6H_4N{=}NC_6H_5)(\mu{-}H)$, **5** formed by the addition of one CO ligand to **4**. Compound **5** loses CO when the CO atmosphere is removed and it is converted back to **4**. Crystals of **5** suitable for X-diffraction analysis were grown by slow evaporation of solvent from a solution under an atmosphere of CO at room temperature. An ORTEP diagram of the molecular structure of **5** is shown in Fig. 3. Compound **5** is structurally similar to **4** except that it contains two terminally coordinated CO ligands, C41-O41 and C42-O42, on the metal atom Ru4, Ru4-C41 = 1.894(4), Ru4-C42 = 1.952(4), instead of one CO ligand as found in **4**. Compound **5** contains a single hydrido ligand that bridges the Ru1 – Ru2 metal-metal bond, $\delta = -21.78$ in the ^{1}H NMR spectrum. Interestingly, the nonbonding Ru1···Ru4 distance in **5** is significantly longer, 3.929(1) Å, than the corresponding distance 3.461(1) Å found in **4**, Ru2···Ru4 = 3.980(1) Å. This can be explained by the differences in the electronic structures of **4** and **5**. The Ru1···Ru4 in **4** is short due to the electronic unsaturation on Ru4. That is, Ru4 is shifted toward Ru1 in order to share partially with some of the electrons on **1**, perhaps nonbonding electrons on that atom. However, the 3.461(1) Å Ru1 – Ru4 distance in **4** is still very long and we would hesitate to describe it as a Ru – Ru single bond. By contrast, atom Ru4 in **5** has a complete 18 electron configuration and it does not need additional electron sharing, so it shifts further away from Ru1 to a very long 3.929(1) Å which we would describe as completely nonbonding. The bond distances to the azobenzene ligand, Ru4-N1 = 2.072(3) Å, Ru4-C1 = 2.111(4) Å are also longer than those found in **4**, but the noncoordinated N=N distance, N1 - N2 = 1.279(4) Å, is virtually the same as that in **4**.

An ADF DFT molecular orbital analysis of **5** was performed in order to compare with the MOs of **4**. Selected MOs for **5** are shown in Fig. 4. The HOMO shows the nature of the bonding of the metalated azobenzene ligand to Ru4. The LUMO shows the lowest energy π^*-orbital in the azobenzene ligand. The HOMO-LUMO gap in **5** is 0.45 eV larger than that in **4**. The LUMO+1 and the LUMO+3 are delocalized orbitals on the Ru_4C portion of the metal cluster. The LUMO+2 is an antibonding orbital concentrated on the Ru3 – Ru4 and the carbide carbon atom. The empty d_z^2-p_z hydrid orbital observed in the LUMO+2 of **4** was not found in **5**.

The reaction of compound **3** with azobenzene in heptane solvent at reflux for 11 h yielded the new azobenzene complex **6** in 68% yield. An ORTEP diagram of the molecular structure of **6** as found in the solid state is shown in Fig. 5. Compound **6** contains a bridging di-σ-η^2-*N*,*N*-coordinated azobenzene ligand across an open edge of an open Ru_5C cluster. The cluster is structurally similar to that found in **4** and **5**. Nitrogen atom N1 of the μ-η^2-*N*,*N*-coordinated azobenzene is coordinated to Ru1 and N2 is coordinated to Ru4, Ru1–N1 = 2.064(4) Å and Ru4–N2 = 2.153(4) Å. The N – N bond distance, N1–N2 = 1.281(5) Å, is still short and indicative of an N – N double bond. This appears to be the first example of a di-σ-μ-η^2-*N*,*N*-coordinated azobenzene ligand. Carty reported an example of a μ_4-η^2-PhNNPh ligand in the complex $Ru_4(CO)_{10}(\mu$-CO)(μ_4-PPh)(μ_4-η^2-PhNNPh) a number of years ago [6a]. In that case, each nitrogen atom was bonded to two Ru atoms and the N – N bond was very long at 1.515(4) Å. Compound **6** contains a η^1–coordinated phenyl group on Ru4, Ru4–C1 = 2.146(5) Å. The gold atom Au1 bridges an edge of the cluster at the Ru1 – Ru2 bond, Ru1–Au1 = 2.7441(5) Å, Ru2–Au1 = 2.8671(5) Å, Ru1–Ru2 = 2.8694(6) Å and the carbene ligand is coordinated to the gold atom Au1, Au1–C60 = 2.058(5) Å. The bridging azobenzene ligand serves as a four electron donor and with 13 CO ligands, one phenyl ligand and one Au(NHC) group, compound **6** achieves a total of 76 cluster valence electrons which is consistent with the observed, opened square-pyramidal structure.

Compound **6** is somewhat similar to the compound $Ru_5(\mu_5$-C)$(CO)_{14}(\mu$-η^2-O=CPh)[μ-Au(NHC)] that was obtained by the addition of CO to compounds **2** or **3** [7].

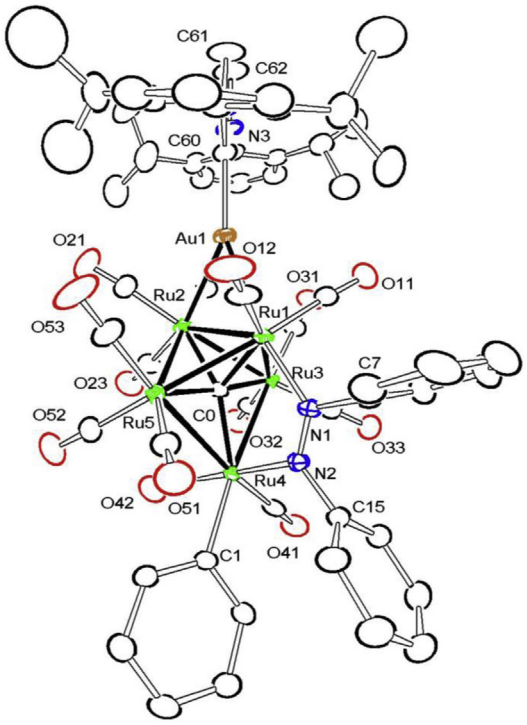

76 electrons

Fig. 5. An ORTEP diagram of the molecular structure of $Ru_5C(CO)_{13}(\mu{-}\eta^2{-}PhN{=}NPh)(\eta^1{-}Ph)[\mu{-}Au(NHC)]$, **6** showing 15% thermal ellipsoid probability. The hydrogen atoms have been omitted for clarity. Selected interatomic distances are (Å) as follow: Ru1–Au1 = 2.7441(5), Ru2–Au1 = 2.8671(5), Ru1–Ru2 = 2.8694(6), Ru1-Ru3 = 2.8167(6), Ru1 – Ru4 = 3.595(1), Ru1-Ru5 = 2.8091(6), Ru2-Ru5 = 2.8201(6), Ru2-Ru3 = 2.8361(6), Ru3-Ru4 - 2.9540(6), Ru4-Ru5 = 2.9649(6), Au1–C60 = 2.058(5), Ru1–N1 = 2.064(4), Ru4–N2 = 2.153(4), Ru4–C1 = 2.146(5), N1–N2 = 1.281(5).

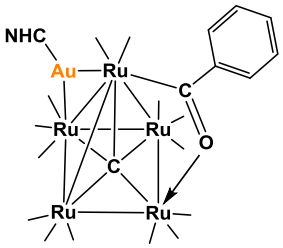

$Ru_5(\mu_5\text{-}C)(CO)_{14}(\mu\text{-}\eta^2\text{-}O{=}CPh)[\mu\text{-}Au(NHC)]$

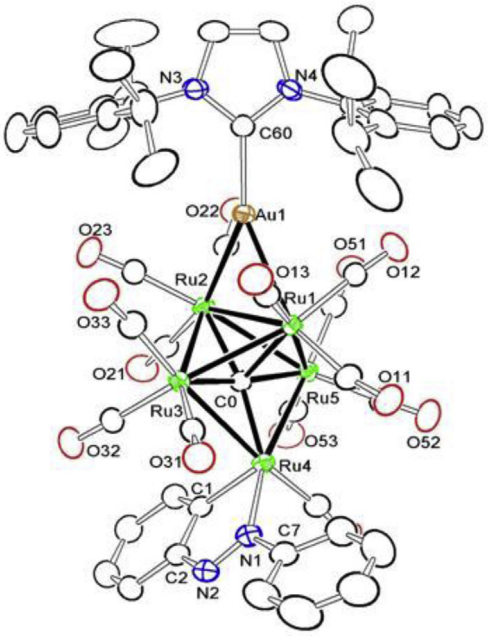

Fig. 6. An ORTEP diagram of the molecular structure of $Ru_5C(CO)_{13}(C_6H_4N{=}NC_6H_5)[\mu{-}Au(NHC)]$, **7** showing 20% thermal ellipsoid probability. The hydrogen atoms in the carbene ligand are omitted for clarity. Selected interatomic distances are (Å) as follows: Ru1–Au1 = 2.7889(5), Ru2–Au1 = 2.8235(5), Ru1···Ru4 = 3.3171(6), Ru1-Ru5 = 2.8047(6), Ru1-Ru3 = 2.8247(6), Ru1-Ru2 = 2.9113(6), Ru2-Ru3 = 2.8506(6), Ru2-Ru5 = 2.8640(6), Ru3-Ru4 = 2.8647(6), Ru4-Ru5 = 2.8621(6), Au1–C60 = 2.040(5), Ru4–N1 = 2.098(5), Ru4–C1 = 1.988(6), N1–N2 = 1.284(6).

When compound **6** was heated to 105 °C for 3 h in a NMR tube in d_8-toluene solvent, the new compound $Ru_5C(CO)_{13}(C_6H_4N{=}NC_6H_5)[\mu{-}Au(NHC)]$, **7** was formed in 19% yield. Compound **7** was also characterized structurally by single-crystal X-ray diffraction analysis. An ORTEP diagram of the molecular structure of **7** is shown in Fig. 6. Compound **7** is very similar to compound **4** except that it contains an Au(NHC) ligand bridging the Ru1 – Ru2 bond of the cluster, Ru1–Au1 = 2.7889(5) Å, Ru2–Au1 = 2.8235(5) Å, Ru1···Ru4 = 3.3171(6) Å instead of a bridging hydrido ligand in the same location in **4**. There is a chelating *ortho*-metalated-azobenzene ligand on the metal atom Ru4. The bonds to this ligand, Ru4–N1 = 2.098(5) Å, Ru4–C1 = 1.988(6) Å, N1–N2 = 1.284(6) Å are very similar to those in **4**. The formation of **7** involved a metalation of one of the phenyl rings of the azobenzene ligand in **6**. The incipient hydrido ligand from the CH activation then combined with the phenyl ligand on Ru4 and benzene was eliminated from the complex. One of the nitrogen atoms of the azobenzene ligand was released from coordination to the metal atoms and the formation of complex **7** was completed following a CO ligand shift to the metal atom Ru2. As result, the total valence electron count on the metal atoms in compound **7** is only 74, and like **4** it is electron deficient by the amount two electrons. As found in **4** the structure of the cluster appears to reflect on this deficiency. Most notably, the Ru1 – Ru4 bond distance has decreased significantly Ru1···Ru4 = 3.3171(6) Å and it is even shorter than the Ru1···Ru4 distance of 3.461(1) Å in **4**. Unfortunately, due to the very small amounts of **7** that we were able to obtain, we were not able to study its reactivity with electron donors such as CO.

4. Summary and conclusions

Summaries of the reactions and products studied in this work are shown in Schemes 1 and 2. The addition of azobenzene to **1** resulted in the formation of the electronically unsaturated compound **4** by the loss of two CO ligands and the addition and metalation of one of the phenyl rings of the azobenzene to the Ru_5 cluster, see Scheme 1. The metal atom containing the metalated azobenzene ligand is formally unsaturated by the amount of two electrons. Although it is weak, there appears to be a significant long-range interaction between the unsaturated metal atom Ru4 and one of the metal atoms is the Ru_4C portion of the cluster. This long-range weak interaction between these two ruthenium atoms is represented by a dashed line shown in the line structure of compound **4** in Scheme 1. In support of its unsaturation character, compound **4** was found to add CO to the metal atom containing the metalated-azobenzene ligand to yield the electronically saturated complex **5**. In the process, the weak interaction between the two ruthenium atoms was eliminated. The CO addition reaction is reversible.

The nature of the addition of azobenzene to compound **3** is shown in Scheme 2. The cluster of **3** opened upon addition of the azobenzene molecule and the bridging phenyl ligand moved to a terminally-coordinated position. The azobenzene ligand adopted a

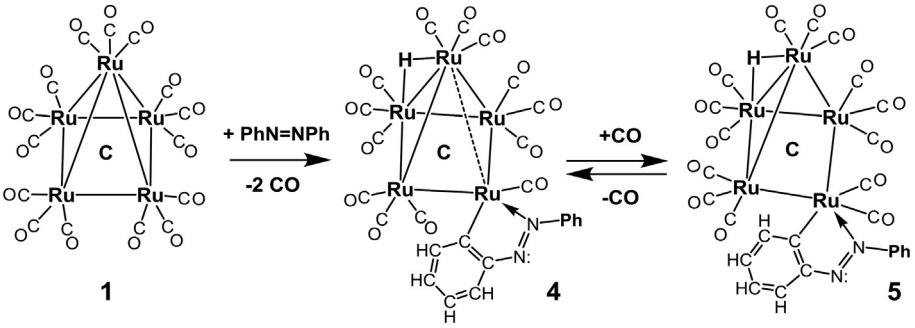

Scheme 1. A schematic of reactions and structures for the compounds **4** and **5** in this study.

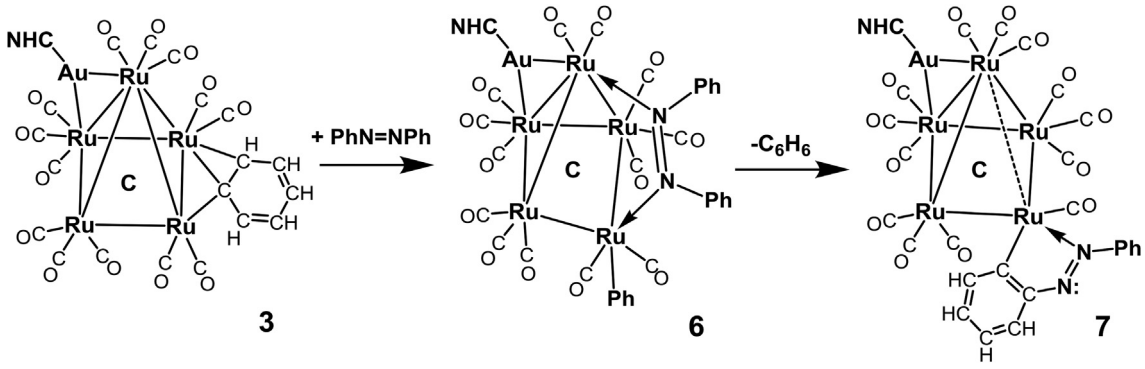

Scheme 2. A schematic of reaction of compound **3** with azobenzene.

bridging di-σ-*N*,*N*-coordination mode in the product **6**. When compound **6** was heated, one of the phenyl rings of the azobenzene ligand became metalated at an ortho-position. The hydrogen atom of the metalated CH bond was shifted to a metal atom where it was combined with the phenyl ligand and benzene was then reductively eliminated from the complex. One of the nitrogen atoms of the azobenzene ligand was released from coordination and the complex became electron deficient, analogous to that of compound **4**. As a result, a weak metal – metal interaction developed between the remote metal atom and one of the metal atoms of the Ru_4C portion of the cluster as represented by the dashed line in the structure of **7** in Scheme 2.

In this work, it has been shown that azobenzene is a viable ligand in Ru_5C cluster complexes. *Ortho*-metallation of a phenyl ring, a common feature of the azobenzene ligand [4], was also observed. Most interestingly, two examples of electronically unsaturated Ru_5 complexes were observed. This property could have implications of additional reactivity toward small donor molecules.

Acknowledgements

This research was supported by grants 1464596 and 1764192 from the U. S. National Science Foundation.

Appendix A. Supplementary data

Supplementary data to this article can be found online at https://doi.org/10.1016/j.jorganchem.2018.10.004.

References

[1] (a) L. Dong, Y. Feng, L. Wang, W. Feng, Chem. Soc. Rev. 47 (2018) 7339–7368; (b) H.M. Dhammika Bandar, S.C. Burdette, Chem. Soc. Rev. 41 (2012) 1809–1825.
[2] (a) R.J. Mart, R.K. Allemann, Chem. Commun. (J. Chem. Soc. Sect. D) 52 (2016) 12262–12277; (b) J. Broichhagen, J.A. Frank, D. Trauner, Acc. Chem. Res. 48 (2015) 1947–1960; (c) A.A. Beharry, G.A. Woolley, Chem. Soc. Rev. 40 (2011) 4422–4437.
[3] W.A. Velema, W. Szymanski, B.L. Feringa, J. Am. Chem. Soc. 136 (2014) 2178–2191.
[4] (a) J.P. Kleiman, M. Dubeck, J. Am. Chem. Soc. 85 (1963) 1544–1545; (b) A.C. Cope, R.W. Siekman, J. Am. Chem. Soc. 87 (1965) 3272–3273.
[5] T.H. Long Nguyen, N. Gigant, D. Joseph, ACS Catal. 8 (2018) 1546–1579.
[6] (a) J.F. Corrigan, S. Doherty, N.J. Taylor, A.J. Carty, J. Chem. Soc., Chem. Commun. (1991) 1640–1641; (b) B. Hansert, H. Vahrenkamp, J. Organomet. Chem. 459 (1993) 265–269.
[7] R.D. Adams, J.D. Tedder, J. Organomet. Chem. 829 (2017) 58–85.
[8] (a) R.D. Adams, J.D. Tedder, Inorg. Chem. 57 (2018) 5707–5710; (b) R.D. Adams, H. Akter, J.D. Tedder, J. Organomet. Chem. 871 (2018) 159–166.
[9] R.D. Adams, J.D. Tedder, Y.O. Wong, J. Organomet. Chem. 795 (2015) 2–10.
[10] B.F.G. Johnson, J. Lewis, J. Nicholls, J. Puga, P.R. Raithby, M. McPartlin, W. Clegg, J. Chem. Soc. Dalton Trans. (1983) 277–290.
[11] SAINT+, Version 6.2a, Bruker Analytical X-ray Systems, Inc., Madison, WI, 2001.
[12] APEX3 Version 2016.5-0 and SAINT Version 8.37A. Bruker AXS, Inc. Madison, WI, USA.
[13] G.M. Sheldrick, SHELXTL, Version 6.1, Bruker Analytical X-ray Systems, Inc., Madison, WI, 1997.
[14] (a) G. te Velde, F.M. Bickelhaupt, S.J.A. van Gisbergen, C. Fonseca Guerra, E.J. Baerends, J.G. Snijders, T. Ziegler, J. Comput. Chem. 22 (2001) 931–967; (b) C. Fonseca Guerra, J.G. Snijders, G. te Velde, E.J. Baerends, Theoret. Chem. Accts. 99 (1998) 391–403; (c) J.P. Perdew, A. Ruzsinszky, G.I. Csonka, O.A. Vydrov, G.E. Scuseria, L.A. Constantin, X. Zhou, K. Burke, Phys. Rev. Lett. 100 (2008) 136406; (d) J.P. Perdew, A. Ruzsinszky, G.I. Csonka, O.A. Vydrov, G.E. Scuseria, L.A. Constantin, X. Zhou, K. Burke, Phys. Rev. Lett. 102 (2009) 039902; (e) E. van Lenthe, E.J. Baerends, J.G. Snijders, J. Chem. Phys. 99 (1993) 4597; (f) E. van Lenthe, E.J. Baerends, J.G. Snijders, J. Chem. Phys. 101 (1994) 9783; (g) E. van Lenthe, A.E. Ehlers, E.J. Baerends, J. Chem. Phys. 110 (1999) 8943; (h) S. Grimme, J. Anthony, S. Ehrlich, H. Krieg, J. Chem. Phys. 132 (2010) 154104.
[15] (a) R.D. Adams, Y. Kan, V. Rassolov, Q. Zhang, Organometallics 730 (2013) 20–31; (b) R.D. Adams, V. Rassolov, Y.O. Wong, Angew. Chem. Int. Ed. 55 (2016) 1324–1327.
[16] G.I. Csonca, A. Ruzisinsky, J.P. Perdew, S. Grimme, J. Chem. Theor. Comput. 4 (2008) 888–891.
[17] R. Koitz, T.M. Soini, A. Genest, S.B. Trickey, N. Rösch, J. Chem. Phys. 137 (2008) 034102.
[18] D.M.P. Mingos, A.S. May, in: D.F. Shriver, H.D. Kaesz, R.D. Adams (Eds.), The Chemistry of Metal Cluster Complexes, VCH Publishers, New York, 1990. Ch. 2.
[19] (a) R.D. Adams, B. Captain, C. Beddie, M.B. Hall, J. Am. Chem. Soc. 129 (2007) 986–1000; (b) R.D. Adams, B. Captain, Angew. Chem. Int. Ed. 44 (2005) 2531–2533; (c) R.D. Adams, B. Captain, L. Zhu, J. Organomet. Chem. 693 (2008) 819–833.